Soft Matter

Accepted Manuscript

ROYAL SOCIETY OF CHEMISTRY

www.rsc.org/softmatter

Unfolding and folding pathway of lysozyme induced by sodium dodecyl sulfate

Yang Sun[a], Pedro L. O. Filho[a], José C. Bozelli Jr.[b], Juliana Carvalho[b], Shirley Schreier[b], Cristiano L. P. Oliveira[a,*]

[a] Instituto de Física, Universidade de São Paulo, Rua do Matão 187, São Paulo-SP, 05314-970, Brasil.

[b] Instituto de Quimica, Universidade de São Paulo, Av. Prof. Lineu Prestes 748, São Paulo-SP, 05508-000, Brasil.

* Corresponding author e-mail: crislpo@if.usp.br

Abstract

Proteins may exhibit unfolding or folding state in the presence of surfactant. In the present work, unfolding and folding pathway of hen egg white lysozyme (HEWL) induced by sodium dodecyl sulfate SDS is studied. The stoichiometry obtained from isothermal titration calorimetry (ITC) provides guidelines for other techniques. The fluorescence spectra and circular dichroism show that fluorescence properties and secondary structure of protein undergo two-step change upon bound with SDS, in which the intensity decrease, emission blue shifts and helical conformation drops in the low ratio of SDS/HEWL, and all of them are back to native like state upon addition of SDS to higher ratio. HEWL presents a higher α-helical content but lost tertiary structure compared to the native state, namely molten state, in the end of binding. Small angle X-ray scattering (SAXS) and the derived model reveal that the complexes possess a novel decorated core-shell structure with the dodecyl chains composing core, and a shell consists of SDS head groups with molten state protein. Five binding steps with individual details involved in the denaturation are obtained to describe the unfolding and folding pathway of HEWL induced by SDS. The results of this work not only present the details of denaturation of protein induced by SDS and structure of complexes involved each binding step, but also provide molecular insights into the mechanism of higher helical conformation of proteins in the presence of surfactant micelles.

INTRODUCTION

The ionic detergent effects solubilization of, for instance, membrane, ribosomal and viral protein is of great interest since these processes may explain important binding mechanisms inside the cell and living systems. Sodium Dodecyl Sulfate (SDS), in particular, has been frequently adopted as a representative anionic surfactant in biophysical and biochemical research. In the presence of SDS, the molecular weight of protein is determined via polyacrylamide gel electrophoresis (PAGE), which is achieved not by the complete unfolding of the proteins but rather by the aggregation of SDS molecules at hydrophobic protein sites. This SDS aggregation induces the so-called "reconstructive denaturation", where proteins adopt a conformational mixture of α-helix and random coil, termed "necklace and bead" structures.[1, 2] The individual micellar "beads" binds to water-soluble proteins approximately in proportion to the polypeptide length, in which, the saturated complexes contain one SDS molecule per two amino-acid residues at moderate ionic strength.[2] An interesting fact found in literature is that globular, water-soluble proteins, as ovalbumin,[3] carbonic anhydrase,[4] α-lactalbumin,[5] pepsin,[6] immunoglobulin G,[6] and fetuin[7] have shown higher helical content in the presence of SDS micelles.

The folding of water-soluble proteins induced by SDS molecules can be applied as a possible approach for a better understanding of the folding mechanisms on globular proteins. The main challenges are: 1) Identify how SDS molecules denature globular protein below and above critical micelle concentration (CMC); 2) what is the structure of complexes in each binding step involved in the denaturation? 3) what is the relationship of SDS-induced helical conformation of protein with SDS micelles? In order to address these questions, in present work, the unfolding and folding pathway of hen egg white lysozyme (HEWL) induced by SDS is reported for the first time, using the isothermal titration calorimetry (ITC), spectra and scattering techniques. Combining with all results, five binding stages involved in the denaturation are obtained to describe the unfolding and folding pathway of HEWL induced by SDS, in

which, a decorated core-shell model expresses structure of complexes in each binding step and clarifies the mechanism of higher helical conformation of protein in the presence of SDS. The outcome of the present work not only helps understand the denaturation of protein induced by SDS and the structure of complexes involved in each binding stage, but also reveals the role of SDS micelles on the unfolding and folding of protein, in general.

EXPERIMENTAL

Experimental section was listed in Supporting Information.

RESULTS

Full view of surfactant binding presented by isothermal titration calorimetry (ITC)

Isothermal titration calorimetry (ITC) directly measures enthalpy change via the heat flow, and it provides the full picture of the different steps of surfactant binding with proteins. In a typical ITC curve, the enthalpic changes are described in terms of changes on the magnitude and sign on the enthalpogram.[8] It also permits the determination of the stoichiometry of binding at each step, which provides a principle guide for investigating the mechanism of protein-surfactant binding and also for the modeling the structure of protein-surfactant complex. Such information can be used on the analysis of scattering data, in particular Small Angle X-ray Scattering (SAXS).

The typical enthalpograms for titration of SDS into HEWL of varying concentrations (0.03-0.15 mM) is listed in Fig. 1, and 11 points along the enthalpogram were selected, corresponding to T1 to T11, which permits the determination of stoichiometry for describing each binding stage.[9] Take the enthalpogram of 0.15 mM HEWL as an example. For the low concentration of SDS (below 1 mM, corresponding to points T1-T2), it shows a strong exothermic peak for ITC curve, which is related to the formation of precipitate due to the neutralization sulfate groups of SDS with positive charged segments of HEWL (Fig. S1, Supporting Information). With the increasing SDS concentration (points T2-T4), the process

accompanies a slightly endothermic peak, followed by a remarkable endothermic behavior, the maximum enthalpy in the whole binding process, is observed between 4-7 mM SDS (points T4-T6). Then an exothermal behavior occurs with a dip at 7–13 mM SDS (points T6 to T10). Beyond this region, the saturated binding of HEWL with SDS molecules and the formation of free micelles present flat enthalpy response (points T10 and T11). Similar behavior is observed for other concentrations of HEWL. It is possible to set a relationship of total SDS concentration [SDS] with bound and free SDS concentration ($[SDS]_{free}$):[10]

$$[SDS]=[SDS]_{free} + N_{Agg}[HEWL] \quad (1)$$

where N_{Agg} is the number of SDS molecules bound per complex, which is a simple linear relation. By selecting 11 points in different transitions defined in Fig. 1A, we have plotted [SDS] as a function of [HEWL] (Fig. 1B), and the free SDS concentration and binding number of different transition points are derived, respectively, from the intercept and slope of Eq.1, and the values of binding parameters are listed in Table 1. The measurements of other techniques were based on the stoichiometry obtained from ITC.

Fluorescence spectra

The fluorescence intensity and emission of HEWL with different ratio of SDS were obtained from the enthalpogram transition points of 0.06 mM HEWL. HEWL contains six tryptophan residues, among them, Trp62, Trp63, Trp108, and Trp123 are exposed to solvent and contribute to the 80% intrinsic fluorescence.[11] As seen from Fig. 2, with the excitation wavelength of 290 nm, HEWL shows an emission peak at 347 nm, it undergoes a two-step change on the SDS binding. Below the ratio of SDS/HEWL of ~85, the intensity decreases and the emission presents a blue shift from 346 nm to 338 nm, and then the intensity increases and the emission shift back to 343 nm upon addition of SDS to higher ratio (~167). Fig. 3A shows the three dimensional fluorescence spectra of native HEWL, and the

parameters are listed in Table S1 (Supporting Information). The peak *a* with the excitation of 290 nm, is contributed by the Trp residues, and the peak *b* with the excitation of 275 nm attributes to the three Tyr residues located in a partially exposed loop region consisted of residues 17-23.[11] The superposition of spectral contributions from several fluorophores, embedded in different local environment, results on a relatively broad fluorescence spectrum for HEWL. Upon binding of SDS from ratio 8 to 85, corresponding to Fig. 3B and 3D, and Table S1, the intensity drops and there is a blue shift of emission for peaks *a* and *b*, and the peak *a* overlaps peak *b* by when changing the ratio of SDS/HEWL 28 to 113. As seen from Fig. 3C to 3F, above ratio of SDS/HEWL 85, all the properties come gradually back to the native like state protein. However, peak *a* shows a 4 nm blue shift for emission comparing native HEWL, and the peak *b* shows ~4 nm blue shift for both of excitation and emission in the end binding of SDS.

Moreover, as seen from the absorption spectra presented in Fig.S2, there is little absorbance for 10 mM pure SDS solution. The absorbance around 270 nm and 280 nm arise and approach maximum at the ratio of SDS/HEWL 85, due to the absorption of precipitation. With increasing ratio of SDS/HEWL, the absorbance decreases attributes to the dissolved precipitates. In addition, in the end binding of SDS, the absorbance increases comparing with native HEWL and the maximum absorption moves little, demonstrating the complexes of SDS/HEWL form.

Circular dichroism analyses

The far-UV CD spectrum of HEWL (0.03 mM) in the presence of different ratio of SDS are shown in Fig. 4A, and the corresponding change in [θ] value at 208 nm and 222 nm as a function of SDS/HEWL ratio are shown in Fig. 4B. The results present that the α-helix of HEWL drops below the ratio of SDS/HEWL 20, and a remarkable increase of the helix content at the ratio of SDS/HEWL 60 is observed, and followed by a small decrease above ratio of SDS/HEWL 80. As seen from Fig. 4C, the helical content reaches a maximum with the ratio of SDS/HEWL 60, stabilizing around 35% while the

fraction of sheet structure drops to 10% and random coil structure maintain around 55%. Similar behavior is observed for 0.01 mM HEWL (data not shown). These demonstrate that protein undergoes loss of helical conformation in the initial association, and it exhibits higher helix content in the end of binding of SDS, clearly indicating unfolding and folding of HEWL induced by SDS. Interestingly, SDS concentrations are below CMC, indicating that the free SDS micelles are not necessary for the higher helical conformation.

The near-UV CD spectra of HEWL with different ratio of SDS are also investigated, in which the region of 290–305 nm, 275–282 nm, and 255–277 nm is contributed by six Trp residues, three Tyr residues and three Phe residues, respectively.[12] As seen from Fig. 4D, SDS bound HEWL shows the characteristic loss of signal, indicating partial unfolding with less restrained aromatic side chains and loss of the tertiary structure. One interesting point is the intensity of the band in the 280-300 nm region increases mildly above ratio of SDS/HEWL 44 shown in Fig. S3, suggesting that a slightly more rigid tertiary structure is recovered comparing with the protein bound with lower ratio of SDS.[13] As seen from Fig. S4, HEWL presents higher helix content but little tertiary structure, namely, molten globule state, in the end binding of SDS.[14-16]

Small angle X-ray scattering (SAXS) identifies SDS–HEWL complexes

Based on the ITC enthalpograms for the titration of SDS into 0.15 mM HEWL, 11 stoichiometric points in five different binding stages were selected to investigate the structure of complexes using SAXS. As seen from Fig. 5A and 5B, the SAXS data and the corresponding $p(r)$ function of native HEWL shows a maximum dimension of 45 Å and a radius of gyration of 16±1Å, which are in good agreement with the known globular structure for the HEWL in solution. The SAXS data of pure 10 mM SDS displays the characteristic bump around q~0.2Å^{-1}, and the $p(r)$ is typical for the micelle structure, showing a positive/negative oscillation, and the maximum diameter of the micelles is around 70 Å.[17]

Increasing the ratio of SDS–HEWL from 2 to 106, the $p(r)$ curves show oscillations in the beginning of curve, and the minimum at ~20Å becomes deeper. As seen from Fig. S5, the comparison of the theoretical scattering intensity of HEWL (calculated from the file 6LYZ.PDB) with the series of experimental data shows that the SAXS experimental data cannot be described above ratio of SDS/HEWL 2. Moreover, the characteristic "bump" is observed for the ratio of SDS/HEWL 7.3. These suggest the formation of complexes of SDS/HEWL with a micelle-like, core–shell structure, despite at such low SDS concentration (1.1 mM).

As the ratio of SDS/HEWL comes to 16.7, a remarkable increase on the scattering intensity is observed at low q while the characteristic "bump" at high q remains, indicating the formation of aggregates ("aggregate **1**") composed of core–shell structure (Fig. S6A). The $p(r)$ shows that the aggregates formed in "aggregate **1**" present globular shape with a maximum diameter of about 600 Å (Fig. S6B). Increasing the ratio of SDS/HEWL to 66, the dissolution of aggregates is triggered by the addition of SDS molecules and the diameter of the complexes declines to about 65 Å. Further, the formation of soluble aggregates ("aggregate **2**") with the core–shell structure is observed by the sample with the ratio of SDS/HEWL 70.7, which is supported by the SAXS data showing the remarkable increase on the intensity at low q and the characteristic "bump" at high q (Fig. S6A). In this case the "aggregate **2**" could also be understood as having a globular shape with maximum diameter of about 500 Å (Fig. S6B), presenting a smaller size and a correspondently lower scattering intensity when compared to "aggregate **1**" initiated by low amounts of SDS. Results from Dynamic Light Scattering (DLS) measurements for "aggregate **1** and **2**" in different concentrations of HEWL are listed in the Fig. S7. The presence of slow components on the correlation curves supports the formation of the aggregates for the above indicate ratios of SDS/HEWL. Interestingly, as seen from Fig. 5A and B, the aggregation is inhibited by increasing the ratio of SDS/HEWL to 86, in which the SAXS data indicates a diameter of about 60 Å.

There are negative portions on the *p(r)* function on this ratio and the free SDS concentration is 4.0 mM (in agreement with the results of conductivity listed in Fig. S8), meaning that the protein-surfactant binding terminates and free micelles of SDS forms.

In order to have a better understanding on the structure of complexes, a decorated core–shell model is used to describe the SAXS data of the ratio of SDS/HEWL 7.3 to 106. One of the main features of the model is the description of the scattering data in absolute scale, with the inclusion of several molecular constraints. Details of the model are listed in the Supporting Information.

As seen from Fig. 5C and Fig. S6C, the model provides a good fitting for all the experimental SAXS data. The modeling results provide the binding number of SDS per complex (N_{Agg}), molecular weight of protein per complex (M_{Prot}) and volume of complex (V), which are displayed in Table 1. It should be noted that the low number of SDS in the initial binding stage leads to a low heat flow, which can reduce the N_{Agg} value obtained by ITC. On the other hand, for samples where the concentration of free SDS is above the CMC, the enthalpy of forming free micelles contributes to the enthalpogram, which increases the N_{Agg} value calculated from ITC. For the ratio of SDS/HEWL of 7.3, the values of N_{Agg} and M_{Prot} obtain from modeling is 7.3 and ~21.61 kD, which is reasonably two HEWL molecules. The V value is ~98543 Å^3 including the contribution of SDS head groups of 2200 Å^3 which is ~3.6 times that of dry HEWL (with dimensions of ~28×32×30 Å and volume of ~26880 Å[18]). The thickness and core radius is 20.41 Å and 8.49 Å with a 74% water fraction. For aggregate **1** with a ratio of SDS/HEWL of 16.7, the radius of gyration of the "aggregate **1**" is ~133 Å with an aspect ratio ε of 2.9, 80% water fraction in the shell, and the average number of decorated micelles forming the complexes is around 40. This number is obtained from the ratio between the volume of aggregates and the volume of the SDS/HEWL complex monomer. The N_{Agg} value is 47 and the free SDS concentration is almost zero, implying that the majority of SDS molecules may be involved in the process of aggregation.

As the ratio of SDS/HEWL increases to 66, the aggregates are disrupted, and the values of M_{Prot}, V and thickness drop to 18.25 kD, 31855 Å^3 and 8.14 Å, respectively, with a 13.42 Å core radius and a water fraction of 44%. For "aggregate **2**" with a ratio of SDS/HEWL 70.7, the radius of gyration of the "aggregate **1**" is ~131 Å with an aspect ratio ε of 1.34 and a water fraction on the shell of 57.3%. For this case one obtains an average number of 120 monomers associated inside aggregates. When the ratio of SDS/HEWL increases to 106, the values of V and M_{Prot} drops to ~36367 Å^3 and 14.38 kD, which approximates to that of native HEWL (26880 Å^3 with 14.4 kD). The thickness is 8.45 Å, which barely corresponds to the thickness of a single α-helix. Also, the N_{Agg} is about 50, which is similar to the ones for free SDS micelle.[19] These demonstrate that the monomer of protein covers almost the full surface area of decorated micelle and micellar core is saturated for SDS molecules in the end of binding. Moreover, the complexes with the ratio of SDS/HEWL 29.3 to 106, corresponding to the T4 to T11, have small variations with a core radius 14.53-14.12 Å, indicating that the micellar core maintains the similar structure.

DISCUSSION

Unfolding and folding pathway of HEWL induced by SDS in different binding stages

Combining the results obtained from all the applied techniques, it is possible to describe the unfolding and folding pathway of HEWL induced by SDS as five stages, as shown in Fig. S9, spanning a broad range of SDS/HEWL ratios. More details are discussed as follows:

Stage 1 (S1, points T1–T2): the sulfate groups of SDS monomers bind to positively charged segments of HEWL (Lys, Arg and His residues), and the neutralization of 8 SDS molecules with 8 net positive charges of HEWL leads to the reduction of the electrostatic repulsion between complexes and precipitation, contributing to the exothermal behavior.[20] Trp62, Trp63, Trp108, and Trp123 are exposed to the solvent, and Trp28 and Trp123 are buried into the hydrophobic interior, being part of the helixes

of 25-28 and 120-125 residues of α-domain, respectively. Trp108 and Trp111 are in the helix-loop-helix domain (87–114 residues) located at the upper lip of the active site cleft region,[21] which may have more motional freedom than other aromatics.[22] With the binding of dodecyl chains of SDS, Trp and Tyr residues are a more hydrophobic environment and less solvent exposure, and the sulfate groups of SDS contacting directly with the π-orbitals of Trp and Tyr residues leads quenching of intensity.[23] The protein is partly unfolded and loss of helical conformation but maintains and overall native shape; there is the exposure of hydrophobic patches, which are now available for the binding with the dodecyl chains of SDS. However, it is difficult to measure the exact penetrating number of molecules in such low ratio of SDS/HEWL, and a reasonable approximation would be 1 or 2 SDS molecules.[24]

Stage 2 (S2, points T2–T4), involves the aggregation and dissolution of neutralized SDS-HEWL complexes. The association of SDS increases electrostatic repulsion and the overall charge of the complex, which promotes the dissolution of the precipitates and induces to a slightly endothermic behavior. The cooperative binding leads to the unfolding of protein, as well as formation of SDS decorated micellar core-shell structures from an uptake of 8 to 25 SDS molecules with an average of two HEWL molecules on the shell sharing the core. The proteins almost fully cover the surface of the decorated micelle, however, parts of proteins may be bound to the decorated micelle, and others may protrude into the solvent. The bound SDS molecules expose their dodecyl chains to the solvent, and it is energetically favorable to form micelle-like structures, even for the number of SDS per complex much lower than the minimum value necessary to form SDS micelles without the presence of the protein.[24] The further accessibility of SDS leads to more hydrophobic environment and quenching of Trp residues, which can be related to the loss of native structure.

Stage 3 (S3, points T4–T6), charge and hydrophobicity play significant roles in this stage, in which additional uptake of SDS to a total of 45 molecules act primarily to unfold the HEWL peptide chain, and

later associate those segments reforming structure with a high helix propensity through electrostatic, internal H-bond and hydrophobic interaction by excluding water.[25] Thus all or most of Trp residues are now located in more hydrophobic environment and the protein presents higher helical content, which leads the more restrictions on the aromatic side chains and the more rigidity of protein upon binding of SDS.[26] The restructuring process contributes to an endothermic behavior and the maximum enthalpy in the whole denaturation.

Stage 4 (S4, points T6–T10): the stripping of HEWL and the recasting of decorated micelles occur in this stage. Being bound to two HEWL molecules, the SDS micellar core is saturated, which initiates the competition of the additional SDS monomers with the decorated micelles for the binding with the protein. The micellar core maintains practically the same radius but it is decorated by a shell with smaller thickness and less amount of protein. It is therefore quite likely that the proteins partially strip from the initial complexes and associate in new decorated micelles. This results in a restructuring protein with a native-like content of secondary structure but little tertiary structure in the transition points T6 to T8. Thus the hydrophobic environment of Trp and Tyr residues decreases slightly and they become partly exposes to solvent with the restructuring of the complexes and the disassociation of dodecyl chains, which induces the Trp residues' intramolecular quenching effects are released and fluorescence intensity is recovered.[27] These are different from the results of Lad's group and Jones's group, who described this stage as being related to the binding of unfolded HEWL with the excess SDS without change of the protein structure and/or formation of clusters.[25, 28]

It is most probable that hydrophobic regions of the partially stripping protein are exposed in this process and act as a driving force for the aggregation process as seen in T9. However, unlike the huge precipitates occur in the initial binding stage predominated by the neutralization, the present aggregation is triggered by the partial stripping protein from the decorated micelle, as described previously. This

probably due to the hydrophobic attraction between the complexes, forming a gel-like, nonviscous solution phase, and the solution phase is of low viscosity containing finite aggregates where the protein is solubilized by micelle-like aggregates.[29, 30] The details of discussion about aggregates are listed in the Supporting Information. Previous studies of SDS/HEWL aggregates indicate that the ratio of surfactant/protein is similar to the one in the present work, and results of atomic-force microscopy (AFM) have shown aggregates with radius of about 200 Å,[31] which is in agreement with "aggregate **2**". The number of decorated micelle inside of "aggregate **2**" increases almost 3 times comparing with that of "aggregate **1**", which is a consequence of the more spherical shape for the decorated micelles forming "aggregate **2**". The aggregates are disrupted later on with increase amount of SDS molecules and dodecyl chains which favors the association of individual micelle like structure, and promotes further stripping of the protein and recast the complexes as SDS micellar core decorated by the monomer of HEWL. The concentration of SDS molecules in the system is high enough to saturate the SDS–protein binding and starts to promote the formation of free micelles. All these mechanisms contribute to the exothermal process.

Stage 5 (S5, points T10–T11): a number of 50 SDS molecules form the micellar core, decorated by monomer protein with a molten globular state. The Trp62, Trp63 and Trp123 residues and Try residues are displaced by dodecyl chains, which leads the less solvent exposure and more hydrophobic environment than the ones found in the native protein.[32] The bulk free SDS micelles form, which also explains the flat enthalpy response of binding saturation. The proposed scheme of the different binding stages of denaturation of HEWL induced by SDS and structure of complexes involved is tentatively displayed in Fig. 6. Although the structural results are based on low resolution SAXS data, it provides an overall impression about the characteristic features of the SDS/HEWL complexes. It is worth to mention that we have not been able to find any other self-consistent model that could fit the data in absolute scale.

In any case, for some curves, the aspect ratio parameter presented some instability during the model optimization.

The role of micelle on unfolding and folding of HEWL

The SDS molecule(s) can penetrate into the hydrophobic core of HEWL, between Ala9, Ala10, His15, Ile88, and Thr89 and its sulfate forms a salt bridge with Lys1.[32] This bridge displaces the salt bridge involving Lys1 and Glu7 in the native HEWL,[33] and consequently dodecyl chains of bound SDS are exposed to the solvent. Therefore, energetically favorable micelle-like structures forms with sufficient space and conformational entropy for the dodecyl chains, the aggregation number has to exceed a minimum value.[24] Since the HEWL backbone decorates at surface of micelle, several hydrophobic patches may be exposed to the solvent. In this way, it is expected that the proteins decorating the micelles interact with other complexes and, depending on the situation, form large aggregates. At higher concentrations of SDS, the hydrophobic patches can bind to SDS which may induce the dissolution of the aggregates. In this view, the SDS can act as an agent of dispersion and solubilization.[24] The unfolded protein allows the dodecyl chains to associate with the exposed hydrophobic residues and also, anchoring the sulfate groups of SDS at the positive charged sites of HEWL, which will create a hydrophobic segment by the exclusion of water. There is considerable evidence that SDS molecule binds to the surface of HEWL and forms a hydrophobic "pocket" by displacing the hydrophobic side chains of Phe38 and Trp123, and positive charged residue of Lys33.[32] This process leads to the stabilization of intramolecular hydrogen bond of HEWL, to the detriment of any intermolecular hydrogen bonding with water.[34] Consequently, a molten globule state of HEWL is accomplished, with a higher helical conformation but little of tertiary structure.

According to Yonath, for the denatured state of HEWL induced by SDS, the α-domain shows somewhat rigidity and the flexibility of the β-domain is observed.[32] The partial helical segment of 8-15 residues of

native HEWL probably acts as a flexible joint and the helical fragment 88-94 folds into a rigid body and hydrophobic residues involved in this segment are displaced; while both of the β-sheet and loop structure maintain its flexibility.[32] In general, since native-like secondary structure is preferentially stabilized in hydrophobic environments, the binding with SDS molecules might lead to the formation of higher structural elements or domains. The majority of higher helical content of HEWL in the presence of SDS molecules is α-helix segment in the native state, and the folding of HEWL induced by SDS can be understood as a result of the cooperative process. This is consistent with previous studies of protein structural transition from the aqueous native state to the "TFE state".[35]

Although the disulfide bonds enhances the stabilization for protein structures by restricting the possible configurations of the chain, they play a small role in folding of protein.[36] The denaturation of HEWL induced by SDS undergoes the separation of the α-domain and β-domain, stretching of fragments and at least one disordered S-S bond from Cys76 to Cys94, which is referred to the “opened” structure.[32] This leads to the expanded maximum dimension when comparing to the one for the native protein (45 Å). Thus, it seems reasonable to assume that the molten globule state HEWL covers almost the full surface area of the decorated micelle in the end of binding.

Conclusion

The combination of the results obtained from all calorimetric, spectral and scattering techniques permitted the retrieval of a new view of the unfolding and folding pathway, and the denaturation mechanism of HEWL induced by SDS, which was not presented in previous works in the literature. The core-shell structure of SDS/HEWL complexes in each binding stage obtained from the modeling of SAXS data in absolute scale, as shown in this work, provides an analysis route that can be used to investigate any kind of protein surfactant complexation.

Acknowledgement

We wish to thank Prof. Teresa Lamy and Dr. Evandro L. Duarte for helping on the collection of the fluorescence spectra. This work is supported by FAPESP, CNPq and inctFCx. The authors acknowledge Prof. Jan Skov Pedersen for providing the FORTRAN code on which the SAXS model was based.

References

1. A. Rath, M. Glibowicka, V. G. Nadeau, G. Chen and C. M. Deber, *Proceedings of the National Academy of Sciences of the United States of America*, 2009, **106**, 1760-1765.
2. Shiraham.K, K. Tsujii and T. Takagi, *Journal of Biochemistry*, 1974, **75**, 309-319.
3. Y. Y. T. Su and B. Jirgensons, *Archives of Biochemistry and Biophysics*, 1977, **181**, 137-146.
4. B. Jirgensons, *Biochimica Et Biophysica Acta*, 1976, **434**, 58-68.
5. W. L. Mattice, J. M. Riser and D. S. Clark, *Biochemistry*, 1976, **15**, 4264-4272.
6. W. Parker and P. S. Song, *Biophysical Journal*, 1992, **61**, 1435-1439.
7. N. Zaidi, S. Nusrat, F. K. Zaidi and R. H. Khan, *Journal of Physical Chemistry B*, 2014, **118**, 13025-13036.
8. D. Otzen, *Biochimica Et Biophysica Acta-Proteins and Proteomics*, 2011, **1814**, 562-591.
9. K. K. Andersen, P. Westh and D. E. Otzen, *Langmuir*, 2008, **24**, 399-407.
10. A. D. Nielsen, L. Arleth and P. Westh, *Biochimica Et Biophysica Acta-Proteins and Proteomics*, 2005, **1752**, 124-132.
11. E. Nishimoto, S. Yamashita, A. G. Szabo and T. Imoto, *Biochemistry*, 1998, **37**, 5599-5607.
12. Sternlic.H and D. Wilson, *Biochemistry*, 1967, **6**, 2881-&.
13. S. M. Kelly and N. C. Price, *Biochimica Et Biophysica Acta-Protein Structure and Molecular Enzymology*, 1997, **1338**, 161-185.
14. K. Kuwajima, *Proteins-Structure Function and Genetics*, 1989, **6**, 87-103.
15. D. T. Haynie and E. Freire, *Proteins-Structure Function and Genetics*, 1993, **16**, 115-140.
16. O. B. Ptitsyn, *Trends in Biochemical Sciences*, 1995, **20**, 376-379.
17. S. Manet, A. Lecchi, M. Imperor-Clerc, V. Zholobenko, D. Durand, C. L. P. Oliveira, J. S. Pedersen, I. Grillo, F. Meneau and C. Rochas, *Journal of Physical Chemistry B*, 2011, **115**, 11318-11329.
18. L. K. Steinrauf, *Acta Crystallographica*, 1959, **12**, 77-79.
19. N. J. Turro and A. Yekta, *Journal of the American Chemical Society*, 1978, **100**, 5951-5952.
20. A. Valstar, W. Brown and M. Almgren, *Langmuir*, 1999, **15**, 2366-2374.
21. H. R. Ibrahim, U. Thomas and A. Pellegrini, *Journal of Biological Chemistry*, 2001, **276**, 43767-43774.
22. G. Zettlmeissl, R. Rudolph and R. Jaenicke, *Biochemistry*, 1979, **18**, 5567-5571.
23. V. Nanda and L. Brand, *Proteins-Structure Function and Genetics*, 2000, **40**, 112-125.
24. K. K. Andersen, C. L. Oliveira, K. L. Larsen, F. M. Poulsen, T. H. Callisen, P. Westh, J. S. Pedersen and D. Otzen, *Journal of Molecular Biology*, 2009, **391**, 207-226.
25. M. D. Lad, V. M. Ledger, B. Briggs, R. J. Green and R. A. Frazier, *Langmuir*, 2003, **19**, 5098-5103.
26. A. I. P. Dekroon, M. W. Soekarjo, J. Degier and B. Dekruijff, *Biochemistry*, 1990, **29**, 8229-8240.
27. D. A. Kelkar, A. Chaudhuri, S. Haldar and A. Chattopadhyay, *European Biophysics Journal with Biophysics Letters*, 2010, **39**, 1453-1463.
28. M. Samso, J. R. Daban, S. Hansen and G. R. Jones, *European Journal of Biochemistry*, 1995, **232**, 818-824.
29. A. K. Moren, M. Nyden, O. Soderman and A. Khan, *Langmuir*, 1999, **15**, 5480-5488.
30. A. Stenstam, A. Khan and H. Wennerstrom, *Langmuir*, 2001, **17**, 7513-7520.
31. S. Kumar, V. K. Ravi and R. Swaminathan, *Biochemical Journal*, 2008, **415**, 275-288.
32. A. Yonath, A. Podjarny, B. Honig, A. Sielecki and W. Traub, *Biochemistry*, 1977, **16**, 1418-1424.
33. S. Daopin, U. Sauer, H. Nicholson and B. W. Matthews, *Biochemistry*, 1991, **30**, 7142-7153.
34. R. Montserret, M. J. McLeish, A. Bockmann, C. Geourjon and F. Penin, *Biochemistry*, 2000, **39**, 8362-8373.
35. M. Buck, S. E. Radford and C. M. Dobson, *Biochemistry*, 1993, **32**, 669-678.
36. S. J. Valentine, J. G. Anderson, A. D. Ellington and D. E. Clemmer, *Journal of Physical Chemistry B*, 1997, **101**, 3891-3900.

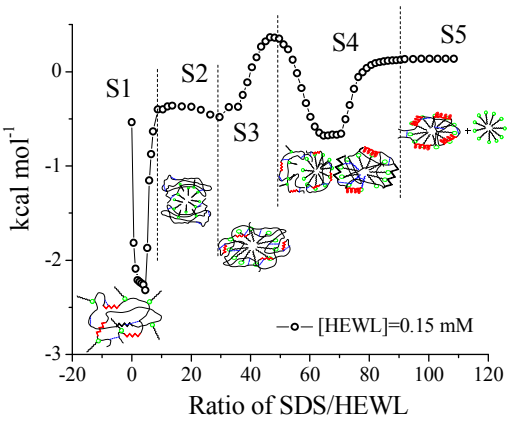

The core-shell structure of complexes in five binding stages involved in the unfolding and folding of lysozyme induced by SDS

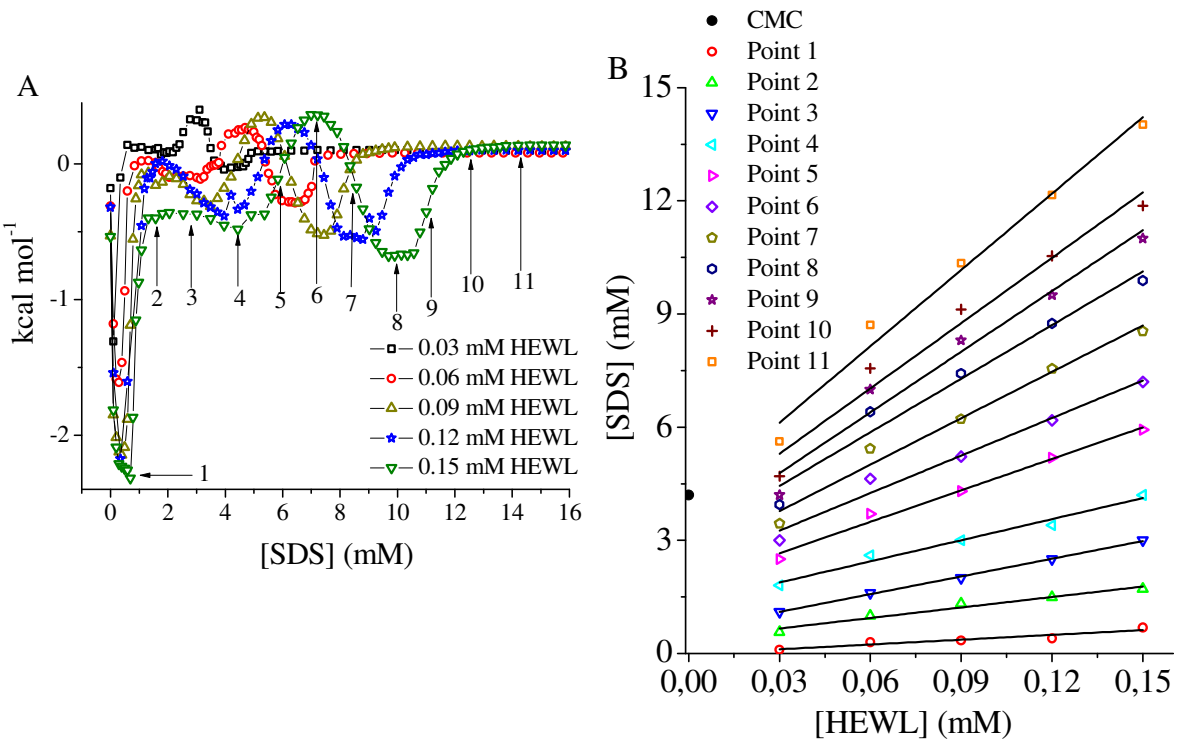

Figure 1. (A): ITC enthalpograms for the titration of SDS (100 mM) into different concentrations of HEWL. On the 0.15 mM HEWL enthalpogram, are indicated the positions where the binding stoichiometry and the free SDS concentration where calculated according to Eq. 1 at different stages of the process. The molecular interpretation of points 1–11 based on spectroscopy and SAXS is discussed in the main text. (B): Total concentrations of SDS, at the different transition points indicated in (A), plotted as a function of HEWL concentration.

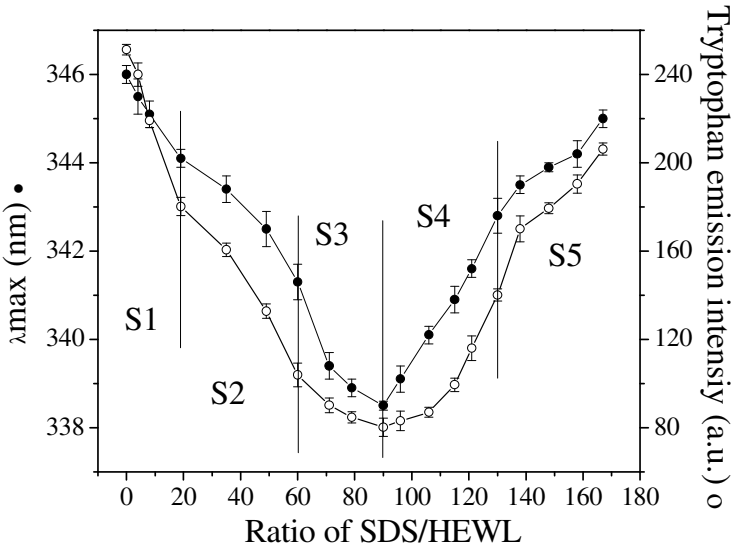

Figure 2. Tryptophan fluorescence intensity and λ_{max} of HEWL with different ratios of SDS, [HEWL]=0.06 mM.

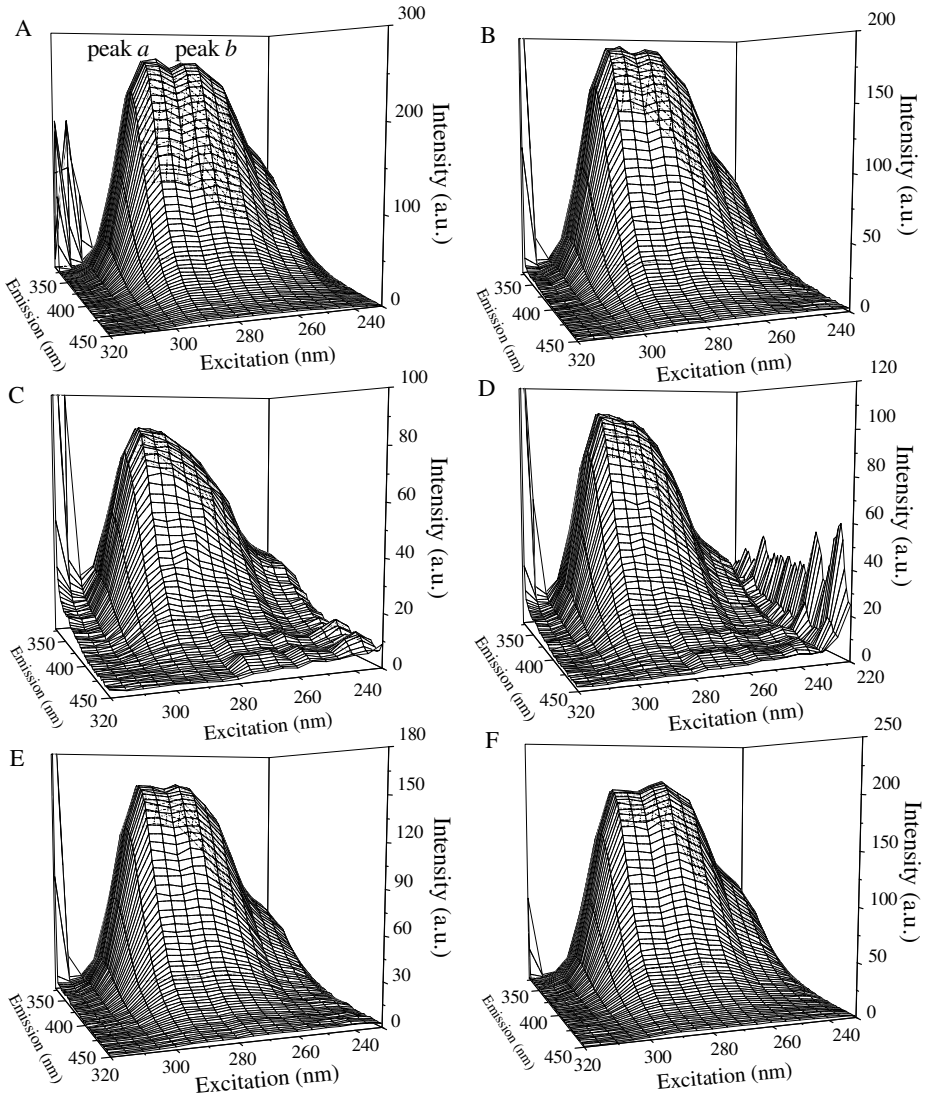

Figure 3. Three dimensional fluorescence spectra of HEWL with different ratios of SDS. (A): native HEWL with the concentration of 0.06 mM; (B) to (F): ratio of SDS/HEWL is 8, 85, 113, 123 and 167, respectively.

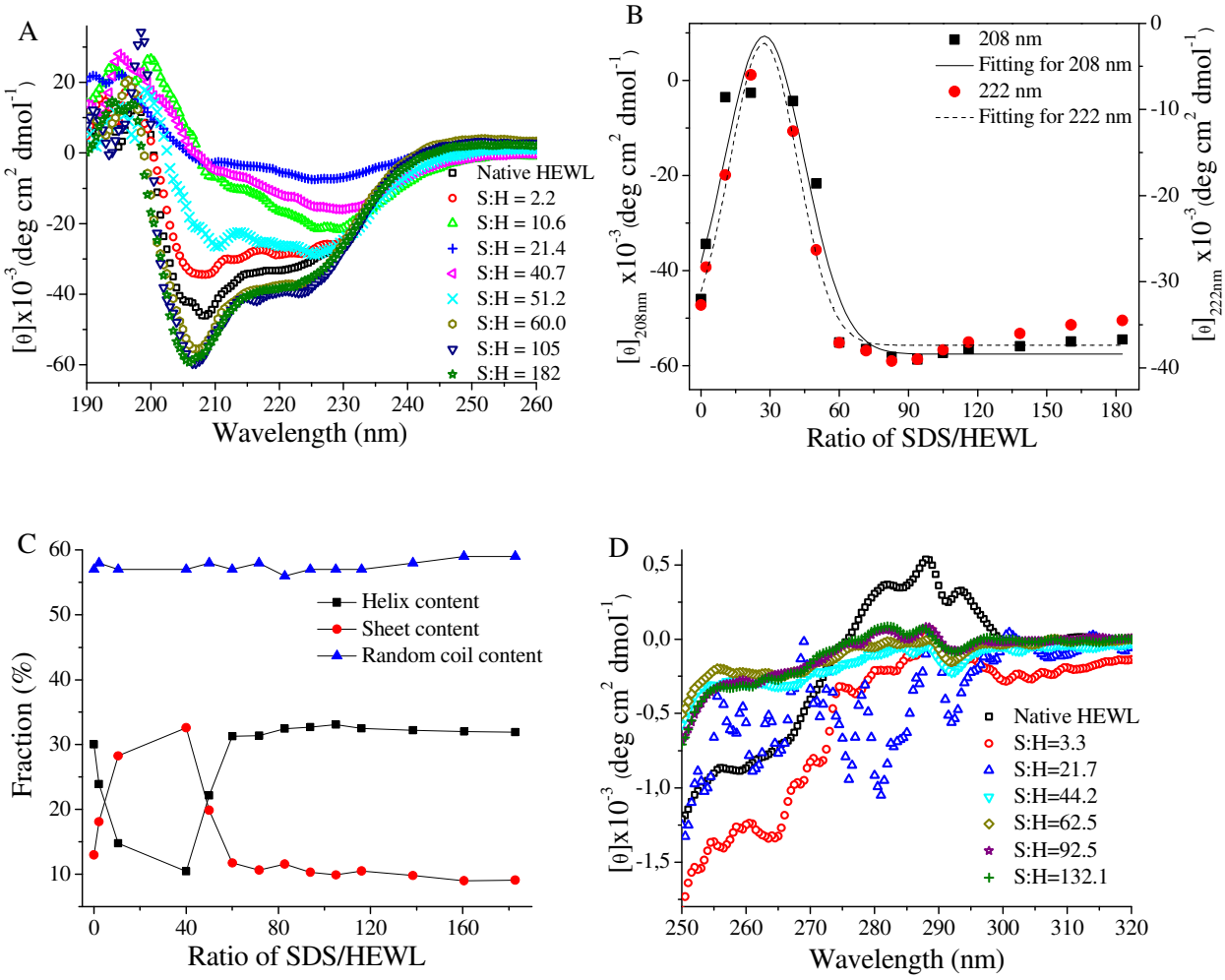

Figure 4. (A) Far-UV CD spectra of 0.03 mM native HEWL in the presence of different ratios of SDS (presented as S:H); (B) Values of [θ] at 208 nm and 222 nm as a function of SDS/HEWL ratios; (C) The fraction of three conformations of 0.03 mM native HEWL with different ratios of SDS/HEWL; (D) Near-UV CD spectra of 0.06 mM native HEWL in the presence of different ratios of SDS. pH = 6.9, T = 20 ℃.

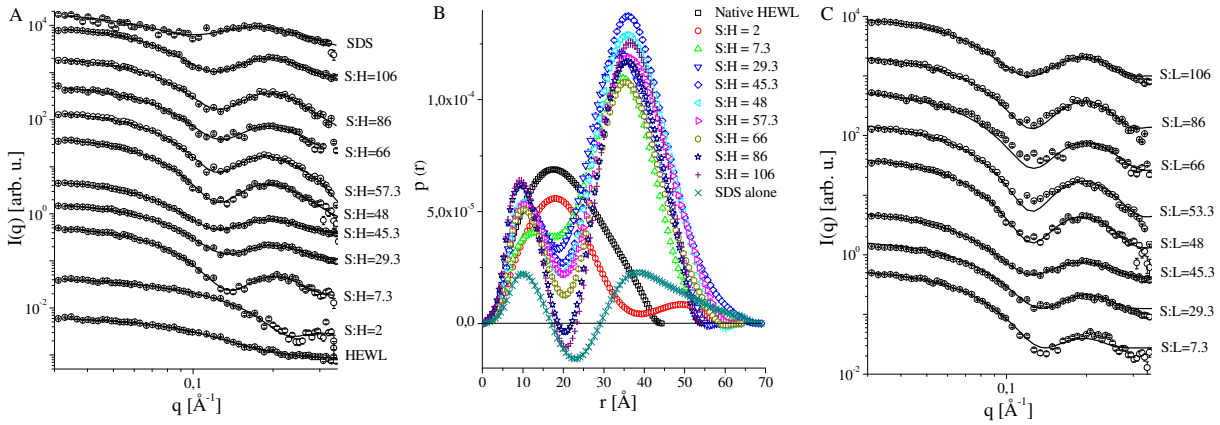

Figure 5 (A): The SAXS results and associated IFT results for selected points. (B): The corresponding pair distance distribution function, $p(r)$. (C): Model fits the data of native HEWL with different ratios of SDS (presented as S:H). The model used, core shell with molten globule, is described at supplementary material. The experimental data are shown as open circles, and the theoretical fits are shown as continuous lines. [HEWL] = 0.15 mM, around 2.2 mg/mL, [SDS] = 0.9-16 mM.

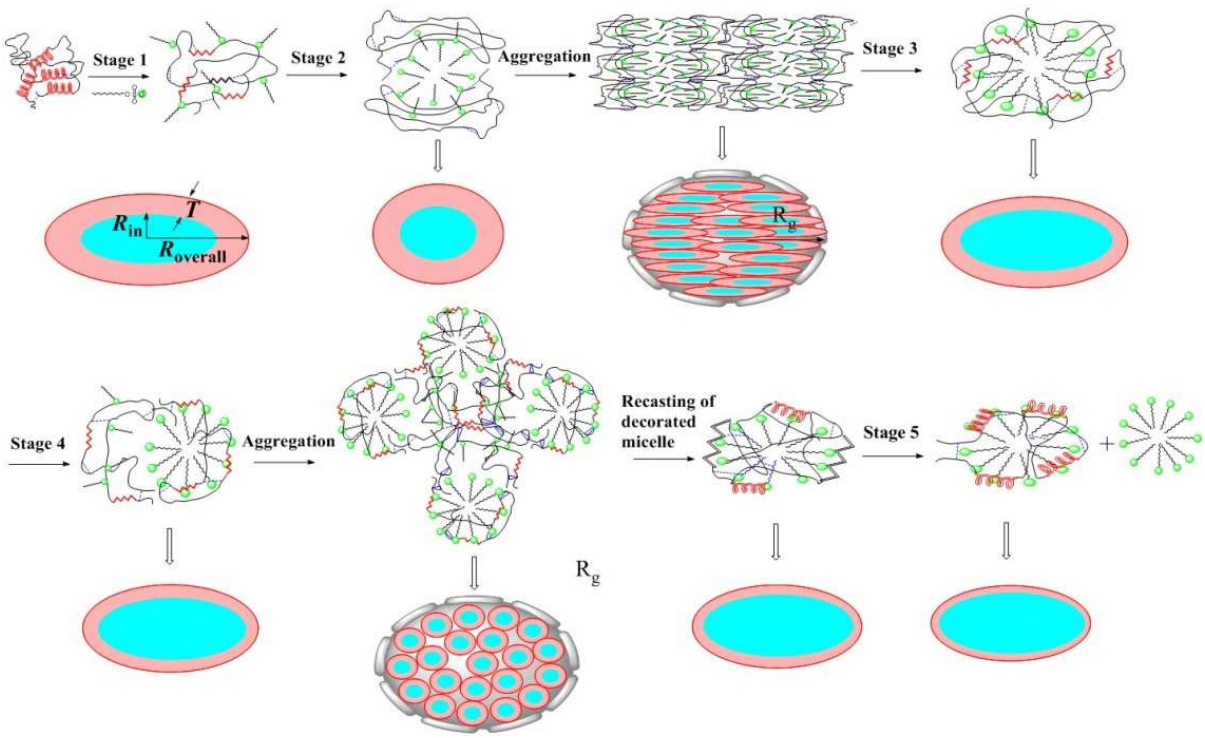

Figure 6: Schematic representation of the different stages of HEWL–SDS binding. Ellipsoidal core-shell structure of radius of core R_{in}, radius of overall R_{over} and shell thickness T, and R_g is the radius of the globular aggregates.

Table 1 Parameters of calculated ITC data and SAXS data modeling of HEWL with different ratios of SDS (presented as S:H).

Selected points (ratio of SDS/HEWL)	Calculation from ITC		SAXS data modeling								
	$[SDS]_{free}$ (mM)	N_{Agg} [a]	T (Å)[#,b]	R_{in} (Å)[#,c]	ε[#,d]	$[SDS]_{free}$[*] (mM)	N_{Agg}[##,a]	F_{water}[##,e] (%)	M_{Prot} (kDa)[##,f]	V[##,g] (Å^3)	χ^2
Native HEWL†	-	-	1.0	11.34	2.86 ± 0.10	-	-	-	14.60	22511	8.0
T1 (S:H=2) †	0	1.9	1.0	9.14	4.46 ± 0.25	-	-	-	14.60	19477	6.7
T2 (S:H=7.3)	0.79	4.9	20.41 ± 0.42	8.49 ± 0.16	1.08 ± 0.30	0.03	7.8	74.1	21.61	98543	10.5
T3 (S:H=16.7), **Aggregate 1**	1.34	10.8	23.75 ± 0.95	11.05 ± 0.25	2.94 ± 0.29	0	47.2	80.0	41.50	-----	45.1
T4 (S:H=29.3)	1.75	19.1	13.34 ± 0.14	14.53 ± 0.22	0.70 ± 0.07	1.9	25.5	58.4	22.45	77828	5.8
T5 (S:H=45.3)	2.23	30.1	10.74 ± 0.09	12.58 ± 0.10	1.93 ± 0.06	2.5	45.7	52.3	23.37	44782	4.3
T6 (S:H=48)	2.39	32.3	10.50 ± 0.12	12.66 ± 0.14	1.90 ± 0.07	2.6	45.7	53.1	21.85	43536	5.9
T7 (S:H=57.3)	2.7	40.0	9.36 ± 0.14	13.02 ± 0.16	1.88 ± 0.09	2.9	49.3	52.0	19.01	37708	12.2
T8 (S:H=66)	3.19	45.5	8.14 ± 0.19	13.42 ± 0.24	1.76 ± 0.12	3.8	50.6	44.1	18.25	31855	12.1
T9 (S:H=70.7), **Aggregate 2**	3.51	47.1	17.79 ± 0.84	12.71 ± 0.37	1.34 ± 0.15	8.8	32.6	57.3	42.83	-----	50.4
T10 (S:H=86)	4.32	60.5	9.00 ± 0.16	13.78 ± 0.27	1.45 ± 0.10	6	45.1	58.0	14.38	38555	11.2
T11 (S:H=106)	4.92	72.7	8.45 ± 0.13	14.12 ± 0.17	1.55 ± 0.07	8	51.7	56.1	14.38	36367	8.05

[HEWL] = 0.15 mM for measurement of SAXS. The volume of HEWL and SDS micelle is 26880 and 415 Å^3, respectively;
[a] Number of SDS molecules per complex;
[b] Thickness of shell;
[c] Core radius;
[d] Aspect ratio of the ellipsoidal object. $\varepsilon = R_{overall}/R_{in}$;
[e] Fraction of water out of the shell;
[f] Molecular weight of protein per complex;
[g] Volume of complex;
[#] Unfixed parameters;
[##] Calculated value;
[*] Fixed parameters;
† Ellipsoidal model;
Aggregate 1 with radius of gyration R_g = 133.4 Å, and **Aggregate 2** with radius of gyration R_g= 131 Å.